Vibrational deexcitation and rotational excitation of H2 and D2 scattered from Cu(111): Adiabatic versus non-adiabatic dynamics

A. S. Muzas, J. I. Juaristi, M. Alducin, R. Díez Muiño, G. J. Kroes, and C. Díaz

Articles you may be interested in

Static surface temperature effects on the dissociation of H2 and D2 on Cu(111)
J. Chem. Phys. 137, 054703 (2012); 10.1063/1.4738956

Theory of vibronic interactions in D2 and H2: A comparison between multichannel-quantum-defect and coupled-equation approaches
J. Chem. Phys. 134, 204305 (2011); 10.1063/1.3593274

Seven-degree-of-freedom, quantum scattering dynamics study of the H 2 D + + H 2 reaction
J. Chem. Phys. 132, 084305 (2010); 10.1063/1.3329730

Theoretical evidence for nonadiabatic vibrational deexcitation in H 2 (D 2) state-to-state scattering from Cu (100)
J. Chem. Phys. 124, 091101 (2006); 10.1063/1.2177664

Adsorption and scattering of H 2 and D 2 by NiAl(110)
J. Chem. Phys. 123, 074705 (2005); 10.1063/1.1999588

Vibrational deexcitation and rotational excitation of H$_2$ and D$_2$ scattered from Cu(111): Adiabatic versus non-adiabatic dynamics

A. S. Muzas,[1] J. I. Juaristi,[2,3,4] M. Alducin,[2,3] R. Díez Muiño,[2,3] G. J. Kroes,[5] and C. Díaz[1,a]

[1]*Departamento de Química Módulo 13, Universidad Autónoma de Madrid, 28049 Madrid, Spain*
[2]*Centro de Física de Materiales (CSIC-UPV/EHU), Materials Physics Center MPC,*
P. Manuel de Lardizabal 5, 20018 San Sebastián, Spain
[3]*Donostia International Physics Center DIPC, P. Manuel de Lardizabal 4, 20018 San Sebastián, Spain*
[4]*Departamento de Física de Materiales, Facultad de Químicas, Apartado 1072, 20080 San Sebastián, Spain*
[5]*Leiden Institute of Chemistry, Gorlaeus Laboratories, Leiden University, P.O. Box 9502, 2300 RA Leiden, The Netherlands*

We have studied survival and rotational excitation probabilities of H$_2$($v_i = 1$, $J_i = 1$) and D$_2$($v_i = 1$, $J_i = 2$) upon scattering from Cu(111) using six-dimensional (6D) adiabatic (quantum and quasi-classical) and non-adiabatic (quasi-classical) dynamics. Non-adiabatic dynamics, based on a *friction* model, has been used to analyze the role of electron-hole pair excitations. Comparison between adiabatic and non-adiabatic calculations reveals a smaller influence of non-adiabatic effects on the energy dependence of the vibrational deexcitation mechanism than previously suggested by low-dimensional dynamics calculations. Specifically, we show that 6D adiabatic dynamics can account for the increase of vibrational deexcitation as a function of the incidence energy, as well as for the isotope effect observed experimentally in the energy dependence for H$_2$(D$_2$)/Cu(100). Furthermore, a detailed analysis, based on classical trajectories, reveals that in trajectories leading to vibrational deexcitation, the minimum classical turning point is close to the top site, reflecting the multidimensionally of this mechanism. On this site, the reaction path curvature favors vibrational inelastic scattering. Finally, we show that the probability for a molecule to get close to the top site is higher for H$_2$ than for D$_2$, which explains the isotope effect found experimentally. © *2012 American Institute of Physics*. [http://dx.doi.org/10.1063/1.4742907]

I. INTRODUCTION

The presence of electronic excitations during the interaction of diatomic molecules with metal surfaces is indisputable. Experiments developed during the last few years have measured, for example, chemicurrents and creation of hot electrons during the chemisorption of atoms and molecules on metal films and surfaces,[1–5] highly efficient multi-quantum vibrational relaxation of highly vibrationally excited NO molecules scattered from metal surfaces,[6,7] and even electron emission upon scattering of highly vibrationally excited NO from a low work function metal surface.[8] Nevertheless, the fundamental question to be answered now is: how much does the presence of electronic excitations influence the interactions between molecules and metal surfaces? And more generally, to what extent can the Born-Oppenheimer approximation (BOA) be used?

The adsorption of O$_2$ on metal surfaces, such as Al(111) (Refs. 9 and 10) and Ag(100),[11] is an intriguing example for which the adiabatic approximation can fail. Behler *et al.* have been able to reproduce the sticking curve of O$_2$ on Al(111) by performing state-of-the-art classical dynamics simulations in which O$_2$ is assumed to remain in an *excited* spin-triplet state along its approach to the surface.[10] Non-adiabatic effects are

also expected in the interaction of surfaces with initially vibrationally excited molecules. Thus, Shenvi *et al.*[12,13] have been able to explain the observed multi-quantum vibrational relaxation of NO scattered from Au(111) using a model that incorporates electron hopping between the surface and the molecule. More recently, low dimensional calculations performed by Monturet *et al.*[14] suggest that an electronic friction model may also account for many of the results obtained in this kind of experiment.

The role of electron-hole (*e-h*) pair excitations is more controversial for the scattering of closed-shell molecules, which are initially in their ground electronic state.[15] Motivated by this controversy, an important number of theoretical methods that include electronic excitations have been recently developed.[16–24] In some cases, non-adiabatic dynamics based on low-dimensional calculations has resulted in overestimation of the effects associated with *e-h* pair excitations. For example, for N$_2$/Ru(0001) it was claimed,[16] based on low-dimensional non-adiabatic calculations, that the huge discrepancy between low-dimensional adiabatic calculations and experiment was mostly due to *e-h* pair excitations, whereas a subsequent adiabatic high-dimensional dynamics study[25,26] showed that most of the discrepancy vanishes when the six degrees of freedom of the molecule are taken into account in the dynamics. Six-dimensional (6D) adiabatic calculations have also been able to reproduce, for instance,

---

a)Electronic mail: cristina.diaz@uam.es.

137, 064707-1

experimental measurements of reactive and non-reactive scattering of H_2 from Pt(111) (Ref. 27) or rotational state distributions of N_2 molecules scattered from W(110).[28] Non-adiabatic 6D dynamics calculations, based on electronic friction coefficients computed with density functional theory (DFT) using different approximations, show that within this approach, *e-h* pair excitations play a minor role in the dissociative adsorption of H_2 on Cu(110), N_2 on various tungsten surfaces, and O_2 on Pd(100).[22,29,30] A similar conclusion has been recently reached for the scattering of N_2 from W(110) and N from Ag(111).[24]

In the particular case of H_2 interacting with copper, adiabatic calculations have been shown to give good results in comparison with experiments for H_2/Cu(100),[31,32] H_2/Cu(110) (Ref. 33), and H_2/Cu(111).[34–36] In fact, for H_2/Cu(111) it has been shown[35,36] that the choice of an appropriate functional in a high dimensional adiabatic calculation leads to a chemically accurate description of experiments on the dependence of reaction on incidence energy and initial rovibrational state, and of experiments on rotationally inelastic scattering. Nevertheless, the role of *e-h* pair excitations in the interaction of H_2 with copper surfaces has been studied not only indirectly through comparison between experiment and adiabatic theory, but also directly through non-adiabatic dynamics calculations. For example, Luntz *et al.*[17] have computed *ab initio* friction coefficients along the reaction path for the dissociative adsorption of H_2 on Cu(111) showing that non-adiabatic effects on dissociative chemisorption are minimal in this case. And Juaristi *et al.*[22] have computed non-adiabatic sticking probabilities for H_2/Cu(110), which closely resemble the adiabatic ones.

Although, as discussed above, non-adiabatic effects have been found to be negligible for several H_2/Cu(111) scattering processes, it has been suggested[37] that they may play a prominent role in the vibrational deexcitation of $H_2(D_2)$ scattered from Cu(100) and Cu(110). Vibrational excitation and deexcitation have been widely studied both theoretically and experimentally. Theoretically, it has been found that London-Eyring-Polyani-Sato (LEPS) potentials[38] may lead to too low vibrational excitation[39] and deexcitation[40] probabilities, which may be attributed to an underestimation of the curvature in the reaction path at surface sites important to vibrationally inelastic scattering.[40] In fact, as shown by Holloway and co.,[41,42] there is a close relationship between the vibrationally inelastic scattering and the presence of a large curvature in the reaction path in front of an especially late barrier. This is the case, for example, for H_2/Cu(100).[43] The influence of surface temperature on vibrationally inelastic scattering has also been studied experimentally[44] and theoretically,[45] suggesting small effects of surface temperature, and therefore, an adiabatic mechanism. On the other hand, Sitz and co.[46] have found that a significant amount of energy in H_2 is lost to the surface upon scattering from Cu(100). Recently,[47] it has been hypothesized, based on an exhaustive analysis of experimental data, that phonons may play a significant role in promoting vibrational excitation.

In summary, there is a considerable evidence that scattering of H_2 from Cu surfaces is not much affected by non-adiabatic effects. Nevertheless, it has been conjectured,[37] based on the comparison between experiment for $H_2(D_2)$/Cu(100) (Refs. 46 and 48) and low-dimensional adiabatic and non-adiabatic theory for $H_2(D_2)$/Cu(111), that the different behavior observed for vibrational deexcitation of H_2 and D_2 represents indirect evidence of a non-adiabatic mechanism. Experiments on vibrational deexcitation of H_2 (Ref. 46) and D_2 (Ref. 48) scattering from Cu(100) show a strong isotope effect in the energy dependence of the vibrational survival probability that exhibits a steeper decrease with incidence energy for H_2 than for D_2. This phenomenon has been considered as an example of a BOA breakdown.[37] This conclusion was based on the comparison between the experimental data of Refs. 46 and 48, and the results obtained for scattering of $H_2(D_2)$ from Cu(111) with non-adiabatic calculations based on a friction model and a three-dimensional potential energy surface (PES). In that 3D PW91-PES, only two degrees of freedom of the molecule (*r* and *Z*) and a single lattice coordinate (to take into account phonons) were included. Therefore, these calculations cannot account for rotational excitation or deexcitation, or for the impact site (X, Y) dependence.

Here, we expand upon the analysis performed by Luntz *et al.*,[37] by performing dynamics calculations on vibrational deexcitation of H_2 and D_2 including all six degrees of freedom of the molecule. Similarly, to Luntz *et al.*,[37] we have used the (111) surface in our analysis, instead of the (100) and (110) surfaces for which scattering of vibrationally excited H_2 was investigated experimentally. We study the (111) surface because an accurate 6D PES for this surface is already available in the literature.[35] Also in view of the rather similar experimental results obtained for the (100) and (110) surfaces, no major discrepancies would be expected between low-Miller-indices Cu surfaces. Keeping in mind that we perform our study for the (111) surface whereas the experiments we compare to were done for the (100) surface, we do not attempt a quantitative comparison with experiment. Rather, the emphasis is on experimental trends, in particular on understanding the isotope effect in the energy dependence of the vibrational survival probability that was also addressed by the work of Luntz *et al.* Our 6D dynamics calculations show that, contrary to what is suggested by low dimensional calculations, the observed difference in this energy dependence between H_2 and D_2 (Refs. 46 and 48) can be qualitatively reproduced by adiabatic calculations if the multidimensionality of the system is taken into account. Inclusion of non-adiabatic effects is not needed to explain this trend. In fact, our analysis shows that the vibrational deexcitation process occurs close to the top site, whereas the previous low dimensional calculations[37] only took into account scattering from the lowest reaction barrier site, the bridge site, explaining the lack of vibrational deexcitation found in the adiabatic calculations presented in Ref. 37. We have also performed non-adiabatic 6D dynamics calculations[22] showing explicitly that *e-h* pair excitations play a very minor role in scattering from Cu(111) in general, and in the isotope effect found experimentally in the energy dependence for $H_2(D_2)$/Cu vibrationally inelastic scattering in particular.

This paper is organized as follows. In Sec. II, we describe briefly the theoretical methods employed. In Sec. III,

we show and discuss our results. And, finally, conclusions are presented in Sec. IV.

II. METHODOLOGY

The theoretical methods used to carry out this study have been described in detail previously, therefore, only a brief summary is provided here. The 6D potential energy surface (PES) (Ref. 49) was obtained by applying the corrugation reducing procedure (CRP) method[50] to a set of density functional theory/generalized gradient approximation (DFT/GGA) data points, sampled throughout the configuration space. In performing the DFT/GGA calculations, we have used the exchange-correlation functional PW91,[51] which yields a semi-quantitative description of the H_2/Cu(111) system.[36] We also show results obtained with the specific reaction parameter (SRP) functional developed by Díaz *et al.*,[35] which has been shown to give chemical accuracy for a significant number of H_2/Cu(111) observables.

Based on these 6D-PESs and within the adiabatic and static surface approximations, we have performed both quantum (Q) (Ref. 52) and quasi-classical (QC) dynamics.[53] State-to-state quantum scattering probabilities have been obtained using a time-dependent wave packet method.[54] In the implementation used,[52] the wave packet is propagated according to the time-dependent Schrödinger equation using the split operator method.[55] The method uses a direct product discrete variable representation (DVR) to represent the dependence of the wave function on the center of mass coordinates (X, Y, Z) and the internuclear distance r (see Fig. 1), and fast Fourier transforms[56] are used to transform the wave function from the DVR to a direct product finite representation (FBR) in momentum space, and vice versa. To represent the dependence of the wave function on the molecular orientation (θ and φ), a non-direct product FBR of spherical harmonics is used. Gauss-Legendre and Fourier transformations are used to switch between the FBR and the DVR representation[57] in θ and φ, respectively, and vice versa. The reflected wave packet is analyzed by computing S-matrix elements using a scattering amplitude formalism.[58]

The QC dynamics refers to the classical approach in which the initial zero point energy of the molecule is included. In general, QC dynamics yields accurate results for activated

FIG. 1. Coordinate system used to define the position and orientation of H_2 relative to the Cu surface.

H_2-surface systems (see, for example, Refs. 36 and 59–63). Within the QC framework, the scattering probabilities, for each initial rovibrational state (v_i, J_i) and initial collision energy, are computed as an average over the molecular initial internal coordinates and internal conjugate momenta, which are obtained through a conventional Monte Carlo sampling method. In order to ensure low statistical errors, we have computed on the order of 10^4 trajectories for each collision energy and rovibrational state. At the end of a classical trajectory, a molecule is considered as scattered whenever the molecule-surface distance (Z) becomes equal to the initial Z distance (5.5 Å), with the molecule's velocity vector pointing towards the vacuum. To assign vibrational and rotational quantum numbers v_f and J_f to a scattered molecule, we evaluate the closest integer that satisfies $J_f = \frac{1}{2}[-1 + (1 + \frac{4L^2}{\hbar})^{1/2}]$, where L is the classical angular momentum, and the closest integer that satisfies $v_f = \frac{S_r}{\pi} - \frac{1}{2}$, S_r being the action variable. We should also point out that to mimic quantum selection rules, according to which only $\Delta J_f = 2$ transition are allowed for diatomic homonuclear molecules, our continuous classical distributions are transformed to discrete representations using the same interval $\Delta J_f = 2$.

Non-adiabatic *e-h* pair excitation effects are incorporated into the QC calculation following the method presented in Refs. 22 and 29. In the following, we will refer these calculations as non-adiabatic. Briefly, for each of the atom constituents of the molecule, a separate friction force proportional to the atom velocity is incorporated in the classical equations of motion. Thus, for each atom, we solve the equation

$$m_i \frac{d^2 \mathbf{r}_i}{dt^2} + \eta(\mathbf{r}_i) \frac{d\mathbf{r}_i}{dt} + \nabla_i V(\mathbf{r}_i, \mathbf{r}_j) = 0, \tag{1}$$

where m_i is the mass of the atom, $\mathbf{r}_i$ is the position along the trajectory, $\nabla_i V(\mathbf{r}_i, \mathbf{r}_j)$ the adiabatic force obtained from the 6D PES, and η is the friction coefficient for each atom, which is calculated within the local density friction approximation (LDFA). In the LDFA, the friction coefficient at each point of the trajectory is approximated by that corresponding to a free electron gas (FEG) with electronic density equal to that of the surface at the point in which the atom is placed. Finally, the friction coefficient for a slow atom traveling through a FEG is obtained from the scattering properties of the Kohn-Sham wave functions in a static density functional theory calculation of the coupled atom-FEG system (see Refs. 22 and 29 and references therein). The model we use to calculate the friction coefficients has been found to be an efficient and sufficiently accurate tool to describe multidimensional adsorbate dynamics driven by hot electrons in an application to femtosecond-laser induced associative desorption of dihydrogen from Ru(0001).[64]

As a result of our simulations, we analyze the final state of the scattered molecules. This allows us to compute the state-to-state scattering probabilities $P(v_i, J_i \rightarrow v_f, J_f)$ from the initial state (v_i, J_i) to the final state (v_f, J_f). The vibrational deexcitation probability, independent of the final rotational state, is defined as

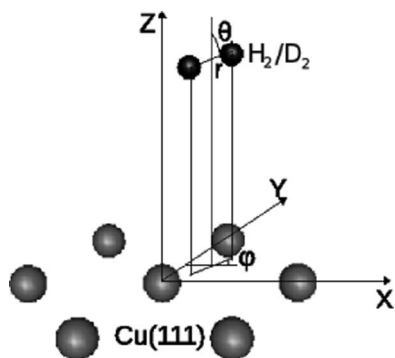$$P_{\text{deex}}(v_i, J_i \rightarrow v_f) = \sum_{J_f} P(v_i, J_i \rightarrow v_f, J_f). \tag{2}$$
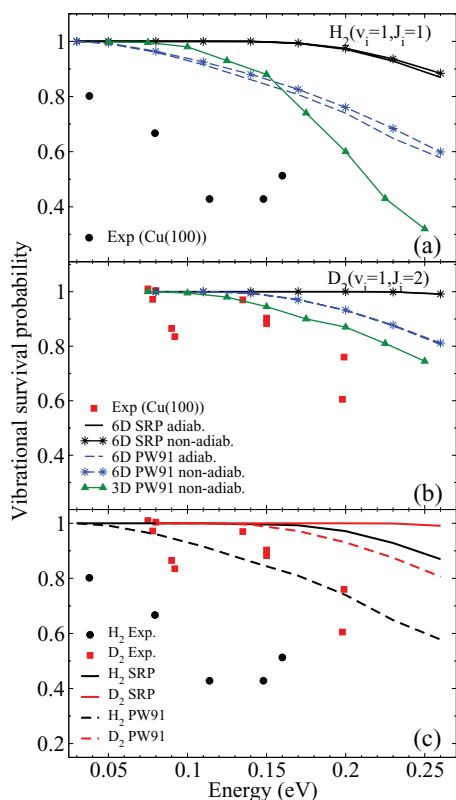
FIG. 2. Vibrational survival probability obtained after considering all possible transitions from $H_2(v_i = 1, J_i = 1)$ to $H_2(v_f = 1, \sum J_f)$ (a) and from $D_2(v_i = 1, J_i = 2)$ to $D_2(v_f = 1, \sum J_f)$ (b) as a function of the incidence energy. H_2 experiment from Ref. 46, D_2 experiment from Ref. 48, and 3D QC non-adiabatic calculations using a PW91-PES, from Ref. 37.

III. RESULTS AND DISCUSSION

In Fig. 2, we compare the experimental vibrational survival probabilities measured for a specific initial H_2 and D_2 rotational quantum number[46,48] with low-dimensional vibrational survival probabilities from Ref. 37, which were meant to describe the transitions $(v_i, J_i) \rightarrow \sum_{J_f} (v_f = v_i, J_f)$, and with our 6D quasi-classical results. The latter results were obtained by summing over all final rotational states and describe transitions from the actual initial rovibrational state, the measurements were done for. From this figure, it can be seen that 6D PW91-PES adiabatic and non-adiabatic results are very similar, and comparable with those obtained from non-adiabatic low-dimensional calculations (3D PW91-PES). The new theoretical calculations show that the vibrational survival probability decreases faster with incidence energy for H_2 than for D_2, as in experiment. At this point, it is worth noticing that the friction coefficients used in our 6D non-adiabatic dynamics are of the same order of magnitude as those computed in Ref. 17 and used in Ref. 37. In Ref. 37, it was claimed that adiabatic dynamics on this 3D PW91-PES predicted no vibrational deexcitation for either H_2, or D_2, and therefore that the isotope effect considered was the result of a non-adiabatic process. However, our 6D adiabatic calculations, showing vibrational deexcitation probabilities higher than zero, and decreasing faster for H_2 than for D_2, contradict this hypothesis. In fact, the lack of vibrational deexcitation obtained in low dimensional adiabatic dynamics calculations should be

considered as an indication of the multidimensionality of the problem, as discussed below.

To fully understand the significance of the results presented in Fig. 2, a few remarks are in order. As emphasized in the Introduction, the aim of this paper is not to quantitatively compare with experiment. Rather, the goal is to show that the isotope effect found for vibrational deexcitation, i.e, its stronger dependence on incidence energy for H_2 than for D_2, can be explained without invoking *e-h* pair excitation processes. There are several reasons that explain why no quantitative agreement between theory and experiment should be expected. Although the comparison between trends in the Cu(100) experiment and the Cu(111) theory is appropriate because no major differences in scattering from the Cu(100) relative to Cu(111) are expected,[37,46] deviations in the absolute values of the measured quantities are to be expected. In fact, this is what we observe when comparing the PW91 and the SRP results in Fig. 2(c): the subtle differences in the PESs change absolute values, but not the qualitative behavior.

We also should take into account that the experiments have been performed at a surface temperature of 500 K, whereas a static surface model has been used to perform our dynamics calculations. Thus, our calculations cannot account for any possible influence of phonon excitations/deexcitations on the survival probabilities. Here, we should point out that although it has been previously shown[65] that including phonons may lead to absolute values in quantitative agreement with experimental data (when the same surface is considered), the qualitative behavior is essentially the same. Therefore, taking into account this fact and the huge computational cost of including, properly, surface motion, in this work, we stick to the use of surface static approximation. Finally, we should take into account the dispersion of the experimental data. Measurements at the same energies show data differing up to 20% (see Figs. 2 and 3). Therefore, as a first approximation, this number could be taken as the experimental error bar. However, even taking this number as error bar, the difference in the energy dependence of survival probabilities between H_2 and D_2 remains.

Figure 2 also shows that the isotope effect in the energy dependence of the survival probability is observed in the 6D simulations independently of the PES used. Both the PW91-PES and the SRP-PES yield qualitatively similar results, i.e., the vibrational survival probability decreases faster with the energy for H_2 than for D_2. This vibrational deexcitation probability is higher for the PW91-PES than for the SRP-PES, which means that subtle differences in the PES, for instance in the barriers heights, may yield quantitatively, though not qualitatively, different results.

Contrary to low dimensional calculations, our 6D simulations also allow one to study the rovibrational survival probabilities actually measured, i.e., the probability that a molecule in an initial quantum state (J_i, v_i) remains in the same state. Rovibrational survival probabilities for $H_2(v_i = 1, J_i = 1)$ and $D_2(v_i = 1, J_i = 2)$ upon scattering from Cu(111) are shown in Fig. 3. In this figure, we show quasi-classical results computed using both adiabatic and non-adiabatic 6D dynamics, and also using two PESs, the PW91-PES, and the SRP-PES. As in the case of vibrational survival probabilities, all
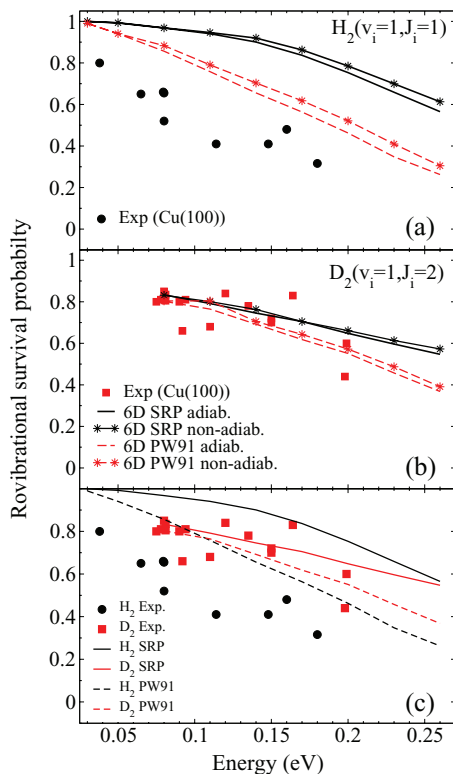
FIG. 3. Rovibrational survival probability for H$_2$(v$_i$ = 1, J$_i$ = 1) (a) and D$_2$(v$_i$ = 1, J$_i$ = 2) (b) as a function of the incidence energy. Experimental data from Refs. 46 and 48. In panel (c), we compare H$_2$ and D$_2$ results.

FIG. 4. Rotational excitation/deexcitation probability as a function of the incidence energy. (a) H$_2$(v$_i$ = 1, J$_i$ = 1) → H$_2$(v$_f$ = 1, J$_f$ = 3); (b) D$_2$(v$_i$ = 1, J$_i$ = 2) → D$_2$(v$_f$ = 1, J$_f$ = 0); (c) D$_2$(v$_i$ = 1, J$_i$ = 2) → D$_2$(v$_f$ = 1, J$_f$ = 4). Black solid circles: experiment from Refs. 46 and 48. Black solid line: 6D QC adiabatic calculations using the SRP-PES; Black solid line with stars: 6D QC non-adiabatic calculations using the SRP-PES; Red dashed line: 6D QC adiabatic calculations using the PW91-PES; Red dashed line with stars: 6D QC non-adiabatic calculations using the PW91-PES.

calculations show the same trend, a faster decrease for H$_2$ than for D$_2$, although the absolute values depend on the PES. For example, the SRP-PES simulations yield absolute values higher for H$_2$ than for D$_2$, whereas the opposite is observed experimentally. Nevertheless, the dependence of the survival probability on the incidence energy, which is the quantity of interest in our analysis, is well reproduced by the SRP-PES results.

In Fig. 4, we compare QC rotational excitation/deexcitation probabilities for H$_2$(D$_2$)/Cu(111) with experimental results for H$_2$(D$_2$)/Cu(100).[46,48] The experimental measurements[46] show an increase of rotational excitation from H$_2$(v$_i$ = 1, J$_i$ = 1) to H$_2$(v$_f$ = 1, J$_f$ = 3) as a function of the incidence energy, from almost 0 at 0.07 eV to 0.06 at 0.2 eV. Our simulated rotational probabilities reproduce qualitatively this experimental trend, although they overestimate this increase. For D$_2$(v$_i$ = 1, J$_i$ = 2), it has been found experimentally[48] that rotational deexcitation from D$_2$(v$_i$ = 1, J$_i$ = 2) to D$_2$(v$_f$ = 1, J$_f$ = 0) does not show a strong dependence on incidence energy, and a similar trend is obtained from our simulations. In this case, it is worth noting that the experimental data might suggest a sharp decrease at low incidence energy, but there is too much noise in the data to make this certain. Finally, rotational excitation from D$_2$(v$_i$ = 1, J$_i$ = 2) to D$_2$(v$_f$ = 1, J$_f$ = 4) has been found, experimentally, to increase with incidence energy, a trend that is also reproduced by our simulations, although once again we overestimate the effect. Here, it should be also taken into account that the classical discretization method (see Sec. II) used to obtain classical state-to-state probabilities tends to
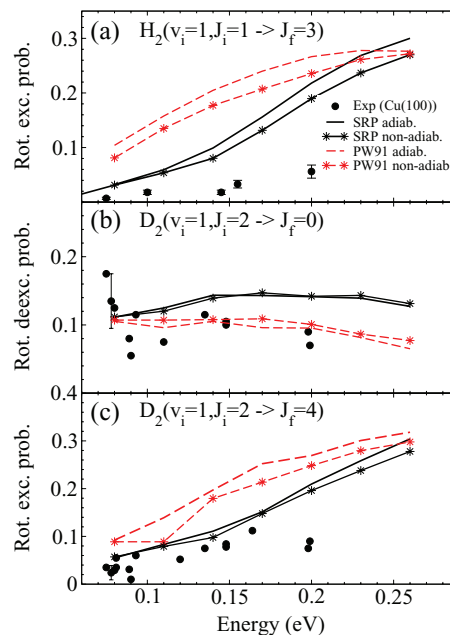
overestimate probabilities for rotationally inelastic scattering, especially for rotational excitation, but also for deexcitation.

To rule out spurious effects on our results due to the use of classical dynamics, we have also performed 6D adiabatic quantum calculations. Quantum survival probabilities for H$_2$ and D$_2$ are shown in Fig. 5. Quantum results resemble the quasi-classical ones, and therefore they also reproduce the
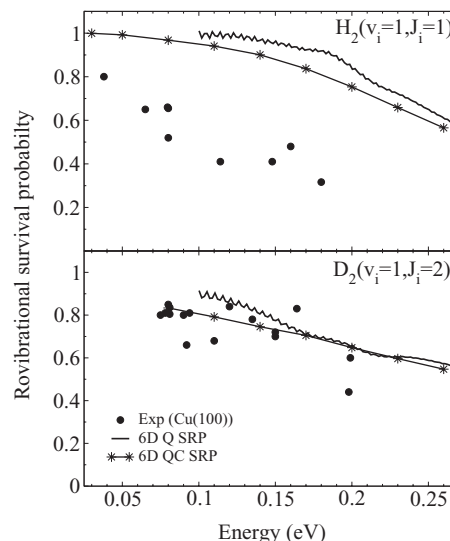

FIG. 5. Rovibrational survival probability as a function of the incidence energy for H$_2$(v$_i$ = 1, J$_i$ = 1) (upper panel) and D$_2$(v$_i$ = 1, J$_i$ = 2) (lower panel). Black solid circles: experiment from Refs. 46 and 48. Black solid line: SRP 6D Q adiabatic calculations. Black solid line with stars: SRP 6D QC adiabatic calculations.
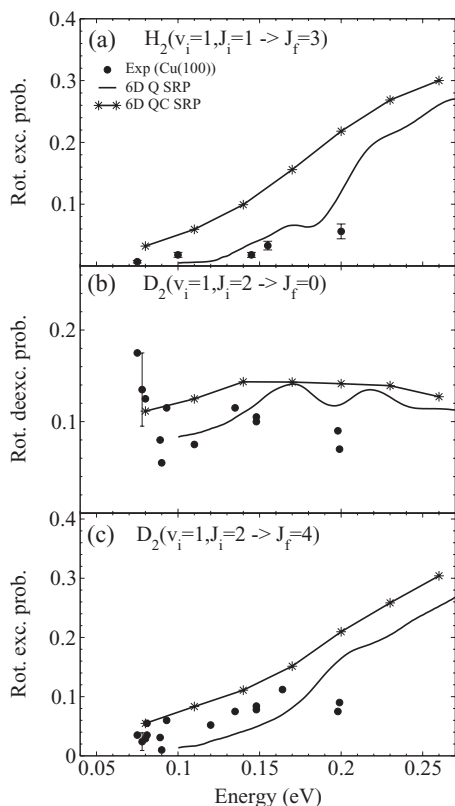
FIG. 6. Rotational excitation/deexcitation probability as a function of the incidence energy. (a) $H_2(v_i = 1, J_i = 1) \rightarrow H_2(v_f = 1, J_f = 3)$; (b) $D_2(v_i = 1, J_i = 2) \rightarrow D_2(v_f = 1, J_f = 0)$; (c) $D_2(v_i = 1, J_i = 2) \rightarrow D_2(v_f = 1, J_f = 4)$. Black solid circles: experiment from Refs. [46] and [48]. Black solid line: SRP 6D Q adiabatic calculations. Black solid line with stars: SRP 6D QC adiabatic calculations.

isotope effect found experimentally. Quantum dynamics also allows one to analyze the rotational excitation (deexcitation) probabilities. From Fig. 6, we can see that rotational excitation from $H_2(v_i = 1, J_i = 1)$ to $H_2(v_f = 1, J_f = 3)$ and from $D_2(v_i = 1, J_i = 2)$ to $D_2(v_f = 1, J_f = 4)$ increases with incidence energy within the energy range where the experimental data were recorded. Quantitative differences between classical and quantum results are due in large part to the classical discretization method (see Sec. II), which tends to overestimate excitation and deexcitation probabilities. Note that the quantum dynamics SRP results are in better agreement with experiment for rotational excitation of $H_2(v = 1, J = 1)$ than the quasi-classical SRP results, and that in some instances, a better agreement of the quasi-classical method with quantum dynamics is obtained for H_2 surface scattering using a discretization procedure based on $\Delta J_f = 1$ binning.[66]

In order to understand the underlying mechanisms behind the isotope effect on $H_2(D_2)$ scattering from low-Miller-indices Cu surfaces, we have analyzed the possible reactive and non-reactive scattering channels for both $H_2(v_i = 1, J_i = 1)$ and $D_2(v_i = 1, J_i = 2)$. The corresponding quantum adiabatic probabilities are shown in Fig. 7. Comparing the two main channels that take away molecules from the initial vibrational state $v_i = 1$, i.e., the reaction and the vibrational deexcitation channels, we can understand the difference for the vibrational survival probabilities between H_2 and D_2.
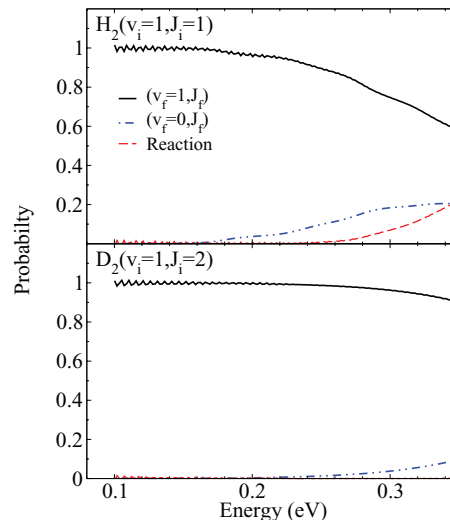

FIG. 7. Reaction probabilities (red dashed line), vibrationally elastic (black line), and inelastic (blue dotted-dashed line) scattering probabilities as a function of the incidence energy. Q calculation using the SRP-PES (upper panel) $H_2(v_i = 1, J_i = 1)$ and (lower panel) $D_2(v_i = 1, J_i = 2)$.

Figure 7 shows that the vibrational deexcitation channel $(v_i = 1, J_i = 1, 2) \rightarrow (v_f = 0, J_f)$ increases faster for H_2 than for D_2 over the whole energy range investigated. Furthermore, for H_2, the reaction probability increases with the incidence energy from zero at 0.16 eV to ≈ 0.2 at 0.35 eV, whereas the reaction probability for D_2 is negligible over the whole energy range. Thus, the results shown in Fig. 7 allow us to understand the experimental observations. The survival vibrational probability decreases faster for H_2 than for D_2 because both the vibrational deexcitation and the dissociation channels are more effective in the former case. At this point, it is worth noting that the experimental upper bounds to the reaction probabilities of H_2 on Cu(100), 0.064 and 0.17 at 0.074 eV and 0.2 eV, respectively,[67] are much higher than the values here computed for Cu(111), which have been found to be close to zero up to about 0.23 eV (see Fig. 7). As noted by the experimentalists,[67]
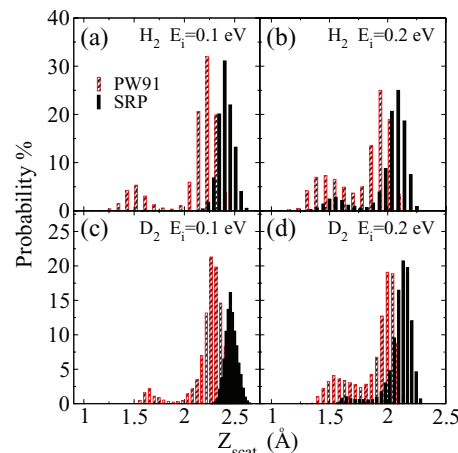

FIG. 8. Distribution of the classical turning point (Z_{scat}) of the molecules scattered from the SRP-PES (solid black bars) and from the PW91-PES (dashed red bars). (a) $H_2(v_i = 1, J_i = 1)$ $E_i = 0.1$ eV; (b) $H_2(v_i = 1, J_i = 1)$ $E_i = 0.2$ eV; (c) $D_2(v_i = 1, J_i = 2)$ $E_i = 0.1$ eV; (d) $D_2(v_i = 1, J_i = 2)$ $E_i = 0.2$ eV.
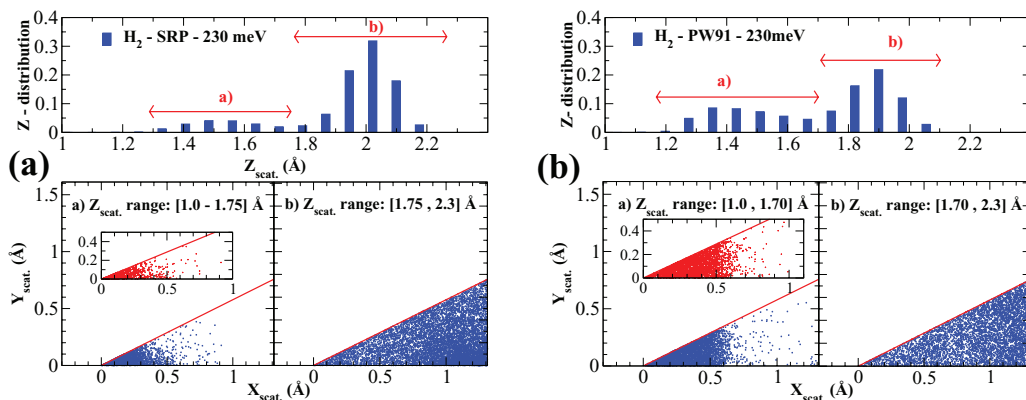
FIG. 9. Top panel: Distribution of the classical turning point (Z_{scat}) of H_2 molecules from the SRP-PES (a) and PW91 (b) for $E_i = 230$ meV. Bottom panel: $X_{cm}Y_{cm}$-distribution of the classical turning point for the scattered H_2 molecules, projected on the irreducible cell (red solid line), for the Z_{scat} intervals marked in the top panel. Insets show $X_{cm}Y_{cm}$-distribution of the vibrationally deexcited molecules.

these experimental results for Cu(100) suggest that, at least, at low energies (≤ 0.2 eV), the vibrational deexcitation channel ($v_f = 0$, $J_f = 1,3$) takes more molecules out of the initial vibrational state than the reaction channel, similarly to our theoretical results for Cu(111) (see Fig. 7).

To further analyze the origin of the difference between H_2 and D_2, we have taken advantage of the classical trajectory method. Our analysis allows us to understand, first, the reason why vibrational deexcitation is more efficient for the PW91-PES than for the SRP-PES. Although the energetic and the geometric corrugation are similar for the two PESs,[49] the PW91-PES presents lower barriers. Therefore, for the same incidence conditions, the molecules get closer to the surface on the PW91-PES (see Fig. 8), which favors the coupling through the curvature of the reaction path from the initial rovibrational state to a different final vibrational state.[41,42] Figure 8 shows that for incidence energies ≥ 0.2 eV, at which the difference between H_2 and D_2 becomes clearly measurable, the H_2 molecules scatter closer to the surface than D_2. This fact may, in principle, explain the isotope effect.

We also observe that the distribution of the classical turning point (Z_{scat}) presents a double peak. The peak closest to the surface in Fig. 8 corresponds to molecules that scatter from the top site, as shown in Fig. 9 for H_2 and Fig. 10 for D_2 for the slightly higher energy of 0.23 eV (this energy

has been chosen to better show the differences between H_2 and D_2). Note that the top site is not the site with the minimum reaction barrier, in fact, the minimum energy reaction barrier for H_2/Cu(111) is located at the bridge site.[49] Thus, Figs. 9 and 10 show that vibrationally excited molecules getting closer to surface do not follow the minimum energy reaction path. This phenomenon has been already described for dissociative adsorption of vibrationally excited H_2 molecules on Cu(100).[68] The top site reaction path for H_2/Cu(111), as in the case for H_2/Cu(100),[43] presents a large curvature in front of the barrier,[49] which promotes vibrationally inelastic scattering.[41,42] Thus, the higher the number of molecules closely approaching the surface and scattered close to the top site, the more vibrational inelastic scattering is expected. If we compare the left bottom panels of Figs. 9 and 10, we see that the number of H_2 molecules scattered from close to the top site, which is at $(X_{cm},Y_{cm}) = (0,0)$, is markedly higher than the number of D_2 molecules scattered from the same site, which explains why vibrational deexcitation is higher for H_2 than for D_2. In fact, the insets in Figs. 9 and 10 show that vibrationally deexcited molecules are always scattered from the nearby top site. This phenomenon is observed independently of the PES, PW91, or SRP. The importance of the top site in the vibrational deexcitation process explains the lack of vibrational deexcitation in the 3D adiabatic calculations by Luntz
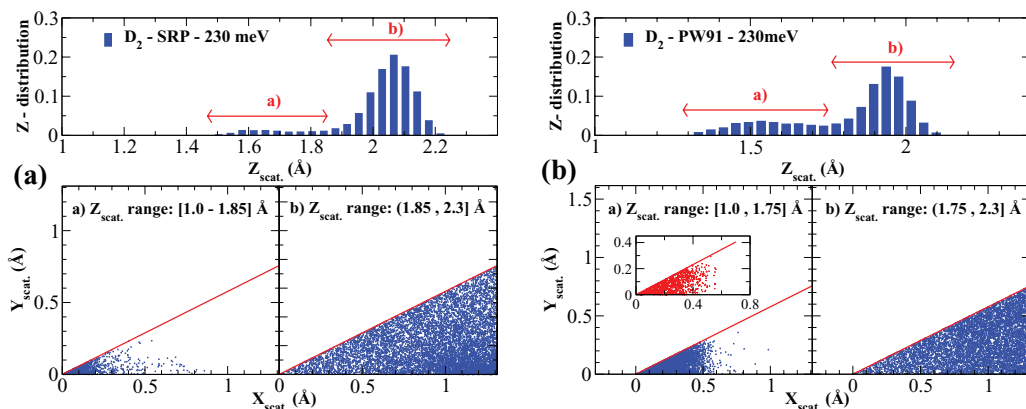

FIG. 10. Similar to Fig. 9, but for D_2.

and co.,[37] who only considered impacts on the bridge site in their calculations.

A question that still remains is why do more H_2 molecules get close to the top site. This phenomenon is linked to vibrational softening, i.e., to the adiabatic energy transfer from the vibrational mode perpendicular to the reaction path to motion along the reaction path. Vibrational energies of H_2 are 1.4 times larger than vibrational energies of D_2, thus, the energy transfer is expected to be higher for H_2 (more energy available) than for D_2, i.e., H_2 molecules may have more energy to get closer to the barriers than D_2. This is the reason why on average, more H_2 molecules get close to the top site. A similar argument has also been used by Sitz and co-workers to rationalise their finding of the larger survival probability for D_2 than for H_2 at equal collision energies.[48]

Finally, it is worth commenting on the experimental results for H_2 at low energy, ($\sim$0.05 eV). The sum of all the rotational channels for $v_f = 1$ was found to be less than 1. In Ref. 46, it was suggested that, disregarding the dissociation channel, this result could be due to a large probability for vibrational relaxation into the states ($v_f = 0$, $J_f = 1$) and ($v_f = 0$, $J_f = 3$). However, our results do not show a significant vibrational deexcitation probability at these low incidence energies. Thus, our results do not support this hypothesis. In fact, the sum of our theoretical rotational probabilities for $v_f = 1$ is equal to 1, no matter the kind of dynamics, quantum or quasi-classical, adiabatic or non-adiabatic; or the functional used. Thus, the question why experimentally the probability for $H_2(v_i = 1, J_i = 1) \rightarrow H_2(v_f = 1, J_f)$ was found to be less than 1, at low energy, remains an open question. At this point, we should also point out that, although it has been suggested that survival and rotational excitation probabilities for $H_2(v_i = 1, J_i = 0)$/Cu(111) are almost independent of surface temperature,[45] quantitative agreement with experiment may require quantum calculations beyond the static surface approximation for the same face of copper as used in the experiments.

IV. CONCLUSIONS

We have performed adiabatic and non-adiabatic six-dimensional (6D) dynamics calculations of vibrational survival and rotational excitation/deexcitation probabilities for $H_2(v_i = 1, J_i = 1)$ and $D_2(v_i = 1, J_i = 2)$ scattering from Cu(111). We have shown that both 6D adiabatic and non-adiabatic dynamics reproduce qualitatively the experimental findings on the similar systems H_2/Cu(100) and D_2/Cu(100), according to which, vibrational survival probabilities decrease with collision energy, the decrease being more pronounced for H_2 than for D_2. Therefore, our results support the idea that energy transfer to electron-hole (*e-h*) pair excitations plays a minor role in the energy dependence of the vibrational deexcitation of H_2 and D_2 scattering from Cu(111).

Our detailed analysis, performed by means of classical trajectories, shows that molecules scattered from close to the top site are responsible for vibrational deexcitation, which is due to the large curvature of the reaction path in front of the top-barrier. We have also shown that the number of molecules scattered from the top site is larger for H_2 than for D_2 be-

cause the amount of energy in vibration available for conversion to motion along the reaction path is larger in $H_2(v_i = 1)$ than in $D_2(v_i = 1)$, which explains the isotope effect found experimentally in the energy dependence of the rovibrational survival probability.

Results presented in this paper also point out the importance of performing multidimensional dynamics, including, at least, all the degrees of freedom of the molecule, in order to understand phenomena such as the isotope effect on rovibrationally inelastic scattering of H_2 from metal surfaces. Low dimensional adiabatic calculations that only consider the reaction path containing the lowest energy barrier geometry (impact on the bridge site) cannot describe a process that occurs predominantly at another site, as shown in our 6D calculations.

[1] H. Nienhaus, H. S. Bergh, B. Gergen, A. Majumdar, W. H. Weinberg, and E. W. McFarland, Phys. Rev. Lett. **82**, 446 (1999).
[2] B. Gergen, H. Nienhaus, W. H. Weinberg, and E. W. McFarland, Science **294**, 2521 (2001).
[3] H. Nienhaus, Surf. Sci. Rep. **45**, 1 (2002).
[4] D. Krix, R. Nünthel, and H. Nienhaus, Phys. Rev. B **75**, 073410 (2007).
[5] E. Hasselbrink, Surf. Sci. **603**, 1564 (2009).
[6] Y. Huang, C. T. Rettner, D. J. Auerbach, and A. M. Wodtke, Science **290**, 111 (2000).
[7] A. M. Wodtke, Y. Huang, and D. J. Auerbach, J. Chem. Phys. **118**, 8033 (2003).
[8] J. D. White, J. Chen, D. Matsiev, D. J. Auerbach, and A. M. Wodtke, Nature (London) **433**, 503 (2005).
[9] K. Honkala and K. Laasonen, Phys. Rev. Lett. **84**, 705 (2000).
[10] J. Behler, B. Delley, S. Lorenz, K. Reuter, and M. Scheffler, Phys. Rev. Lett. **94**, 036104 (2005).
[11] M. Alducin, H. F. Busnengo, and R. Díez-Muiño, J. Chem. Phys. **129**, 224702 (2008).
[12] N. Shenvi, S. Roy, P. Parandekar, and J. C. Tully, J. Chem. Phys. **125**, 154703 (2006).
[13] N. Shenvi, S. Roy, and J. C. Tully, Science **326**, 829 (2009).
[14] S. Monturet and P. Saalfrank, Phys. Rev. B **82**, 075404 (2010).
[15] R. Cooper, I. Rahinov, Z. Li, A. Matsiev, D. J. Auerbach, and A. M. Wodtke, Chem. Sci. **1**, 55 (2010).
[16] L. Diekhöner, L. Hornekaer, H. Mortensen, E. Jensen, A. Baurichter, V. V. Petrunin, and A. C. Luntz, J. Chem. Phys. **117**, 5018 (2002).
[17] A. C. Luntz and M. Persson, J. Chem. Phys. **123**, 074704 (2005).
[18] M. Lindenblatt and E. Pehlke, Phys. Rev. Lett. **97**, 216101 (2006).
[19] M. S. Mizielinski, D. M. Bird, M. Persson, and S. Holloway, J. Chem. Phys. **126**, 034705 (2007).
[20] H. Cheng, N. Shenvi, and J. C. Tully, Phys. Rev. Lett. **99**, 053201 (2007).
[21] D. M. Bird, M. S. Mizielinski, M. Lindenblatt, and E. Pehlke, Surf. Sci. **602**, 1212 (2008).
[22] J. I. Juaristi, M. Alducin, R. Díez-Muiño, H. F. Busnengo, and A. Salin, Phys. Rev. Lett. **100**, 116102 (2008).
[23] M. Timmer and P. Kratzer, Phys. Rev. B **79**, 165407 (2009).
[24] L. Martin-Gondre, M. Alducin, G. A. Bocan, R. Díez-Muiño, and J. I. Juaristi, Phys. Rev. Lett. **108**, 096101 (2012).
[25] C. Díaz, J. K. Vincent, G. P. Krishnamohan, R. A. Olsen, G. J. Kroes, K. Honkala, and J. K. Nørskov, Phys. Rev. Lett. **96**, 096102 (2006).

[26] C. Díaz, J. K. Vincent, G. P. Krishnamohan, R. A. Olsen, G. J. Kroes, K. Honkala, and J. K. Nørskov, J. Chem. Phys. **125**, 114706 (2006).

[27] P. Nieto, E. Pijper, D. Barredo, G. Laurent, R. A. Olsen, E. J. Baerends, G. J. Kroes, and D. Farías, Science **312**, 86 (2006).

[28] K. R. Geethalakshmi, J. I. Juaristi, R. Díez-Muiño, and M. Alducin, Phys. Chem. Chem. Phys. **13**, 4357 (2011).

[29] I. Goikoetxea, J. I. Juaristi, M. Alducin, and R. Díez-Muiño, J. Phys.: Condens. Matter **21**, 264007 (2009).

[30] J. Meyer and K. Reuter, New J. Phys. **13**, 085010 (2011).

[31] D. A. McCormack, G. J. Kroes, R. A. Olsen, J. A. Groeneveld, J. N. P. van Stralen, E. J. Baerends, and R. C. Mowrey, Faraday Discuss. **117**, 109 (2000).

[32] E. Watts, G. O. Sitz, D. A. McCormack, G. J. Kroes, R. A. Olsen, J. A. Groeneveld, J. N. P. van Stralen, E. J. Baerends, and R. C. Mowrey, J. Chem. Phys. **114**, 495 (2001).

[33] G. J. Kroes, E. Pijper, and A. Salin, J. Chem. Phys. **127**, 164722 (2007).

[34] J. Dai and J. C. Light, J. Chem. Phys. **107**, 1676 (1997).

[35] C. Díaz, E. Pijper, R. A. Olsen, H. F. Busnengo, D. J. Auerbach, and G. J. Kroes, Science **326**, 832 (2009).

[36] C. Díaz, R. A. Olsen, D. J. Auerbach, and G. J. Kroes, Phys. Chem. Chem. Phys. **12**, 6499 (2010).

[37] A. C. Luntz, M. Persson, and G. O. Sitz, J. Chem. Phys. **124**, 091101 (2006).

[38] J. Dai and J. C. Light, J. Chem. Phys. **102**, 6280 (1995).

[39] M. F. Somers, S. M. Kingma, E. Pijper, G. J. Kroes, and D. Lemoine, Chem. Phys. Lett. **360**, 390 (2002).

[40] S. Nave, D. Lemoine, M. F. Somers, S. M. Kingma, and G. J. Kroes, J. Chem. Phys. **121**, 214709 (2005).

[41] G. R. Darling and S. Holloway, J. Chem. Phys. **97**, 734 (1992).

[42] G. R. Darling and S. Holloway, Surf. Sci. **307–309**, 153 (1994).

[43] G. J. Kroes, G. Wiesenekker, E. J. Baerends, and R. C. Mowrey, Phys. Rev. B **53**, 10397 (1996).

[44] C. T. Rettner, H. A. Michelsen, and D. J. Auerbach, Chem. Phys. **175**, 157 (1993).

[45] T. Sahoo, S. Sardar, P. Mondal, B. Sarkar, and S. Adhikari, J. Phys. Chem. A **115**, 5256 (2011).

[46] E. Watts and G. O. Sitz, J. Chem. Phys. **114**, 4171 (2001).

[47] G. J. Kroes, C. Díaz, E. Pijper, R. A. Olsen, and D. J. Auerbach, Proc. Natl. Acad. Sci. U.S.A. **107**, 20881 (2010).

[48] L. C. Shackman and G. O. Sitz, J. Chem. Phys. **123**, 064712 (2005).

[49] C. Díaz, R. A. Olsen, H. F. Busnengo, and G. J. Kroes, J. Phys. Chem. C **114**, 11192 (2010).

[50] H. F. Busnengo, A. Salin, and W. Dong, J. Chem. Phys. **112**, 7641 (2000).

[51] J. P. Perdew, J. A. Chevary, S. H. Vosko, K. A. Jackson, M. R. Pederson, D. J. Singh, and C. Fiolhais, Phys. Rev. B **46**, 6671 (1992).

[52] E. Pijper, G. J. Kroes, R. A. Olsen, and E. J. Baerends, J. Chem. Phys. **117**, 5885 (2002).

[53] M. Karplus, R. N. Porter, and R. D. Sharma, J. Chem. Phys. **43**, 3259 (1965).

[54] R. Kosloff, J. Phys. Chem. **92**, 2087 (1988).

[55] M. D. Feit, J. J. A. Fleck, and A. Steiger, J. Comput. Phys. **47**, 412 (1982).

[56] D. Kosloff and R. Kosloff, J. Comput. Phys. **52**, 35 (1988).

[57] G. C. Corey and D. Lemoine, J. Chem. Phys. **97**, 4115 (1992).

[58] R. C. Mowrey and G. J. Kroes, J. Phys. Chem. **103**, 1216 (1995).

[59] D. A. McCormack and G. J. Kroes, Phys. Chem. Chem. Phys. **1**, 1359 (1999).

[60] G. J. Kroes, Prog. Surf. Sci. **60**, 1 (1999).

[61] E. Pijper, M. F. Somers, G. J. Kroes, R. A. Olsen, E. J. Baerends, H. F. Busnengo, A. Salin, and D. Lemoine, Chem. Phys. Lett. **347**, 277 (2001).

[62] G. J. Kroes and M. F. Somers, J. Theor. Comput. Chem. **4**, 493 (2005).

[63] P. Rivière, H. F. Busnengo, and F. Martín, J. Chem. Phys. **123**, 74705 (2005).

[64] G. Fuchsel, T. Klamroth, S. Monturet, and P. Saalfrank, Phys. Chem. Chem. Phys. **13**, 8659 (2011).

[65] F. Nattino, C. Díaz, B. Jackon, and G. J. Kroes, Phys. Rev. Lett. **108**, 236104 (2012).

[66] H. F. Busnengo, W. Dong, P. Sautet, and A. Salin, Phys. Rev. Lett. **87**, 127601 (2001).

[67] K. Jonghyuk and G. O. Sitz, Mol. Phys. **108**, 1027 (2010).

[68] D. A. McCormack, G. J. Kroes, R. A. Olsen, J. A. Groeneveld, J. N. P. van Stralen, E. J. Baerends, and R. C. Mowrey, Chem. Phys. Lett. **328**, 317 (2000).